Diyala Journal of Engineering Sciences

Journal homepage: https://djes.info/index.php/djes

ISSN: 1999-8716 (Print); 2616-6909 (Online)

# Predicting of Seismic Performance on Tunnel in Weak Soil

Nuha J. Najm[1,*], Waad A. Zakaria[1] and Muftah Mohamed Sreh[2]

[1]Department of Civil Engineering, University of Diyala, 32001 Diyala, Iraq
[2]Departement of Civil Engineering, University of Elmergib, Al-Khoms, Libya

**ARTICLE INFO**

***Article history:***
Received June 1, 2022
Revised December 19, 2022
Accepted December 23, 2022
Available April 14,2023

***Keywords:***
Tunnel
Weak soil
FEM analysis

**ABSTRACT**

Main seismic situations have appeared that the tunnels in weak soil may be suffer large seismic damage. Suitable modeling can have great significance for predicting and estimating their seismic acting. This paper examines the effect of the tunneling process and the seismic effect on the tunnel model and the surrounding soil on it. The data of this research is from Almafraq overhead intersection project in the Diyala government, the soil consists of clay and sand layers in which the tunnel is set up. The data obtained from field and laboratory investigations of soil layers and the analysis of the tunneling model by three-dimensional finite element analyses using PLAXIS 3D (V 20), the Mohr-Coulomb (MC) model is employed to demonstrate the behavior of soil-structure interaction in a soil tunnel. Plastic counting was used to act as an elastic-plastic distortion. Three sections are chosen in the vertical direction to experiment with the tunnel's impact and seismic effect on nearby soils. From proceeding FE analysis, the results of calculation by math measurement appeared to main variations in stresses that happen in soils zones nearby the tunnel edges and below the tunnel essentially affect nearness to soils. The increasing pressure becomes smaller as much as you went away horizontally from the tunnel and start to decrease for lengths more than 15m from the tunnel edge's, so it was observed that the most probable safe distance (2D) from the tunnel, which D represents the diameter of the tunnel, this for tunneling. Also, the upper zone of the tunnel considers safer at 58% because it is far from the influence of the earthquake and its soil is clay, while the critical zone locates in contact with the tunnel. Furthermore, it was noted that the amount of settlement of the soil is so little in a phase of tunnelling compared to the dynamic rate of 86%.

## 1. Introduction

Tunnels are considered one of the majority significant means of transmission underground. It is useful in the construction area where no more roofs can be created to confirm the huge traffic infrastructure. Second, it also provides a fast, continuous flow between the points. So largely populated cities around the world are presently designing to supply metro lines by means of a system called an underground tunnel system. Though it has numerous useful goals, it is also at the same interval subject to too much damage if it is located in an earthquake-prone zone [1].

The progress of underground urban infrastructure has become a major focus, with the increase in the population of major cities in the world. The dynamic restrain for underground structures to seismic loads should be specified to lower economic deterioration and warn human safety, if these structures are established in earthquake zones. While the above-ground structures such as tunnels, which are highly contained are dissimilar since it is designed based on the reality that earthquakes

* Corresponding author.
E-mail address: Eng_Grad_civil030@uodiyala.edu.iq
DOI: 10.24237/djes.2023.16202

appear as inertial forces and result in fundamental distortion of the soil structure. Previously, engineers believed that earthquakes caused less damage to underground structures than surface structures, but earthquakes in the 1990s caused massive damage to tunnels, forcing a reassessment of this view. In recent years, there have been numerous examples in different countries of earthquakes causing massive damage to underground structures (for example, the Kobe earthquake, 1995; Taiwan, 1999) [2] indicating that it is crucial to conduct studies on tunnel seismic behavior.

Recently researchers concentrate on the seismic behavior of the tunnels in various kinds of soil. Wang [3], Penzien [4], and Bobet [5] advanced closed-form option of solutions to assess the seismically moments and forces in different tunnels resulting the types of failure like racking and ovaling.

The depth of digging for the tunnel beneath the ground, the sort of soil that surrounds all sides of the tunnel, extreme ground acceleration, the strength of the earthquake, and the distance of the tunnel to the earthquake epicenter represent the factors that affect the tunnels under dynamic loading. Many researchers have attituded the experimental and numerical studies on various sides of seismic action of underground infrastructures, by considering the significance of the object. several numerical studies, like as Hashash et al., [6]; Huo et al., [7]; Anastasopoulos et al., [8, 9]; Amorosi and Boldini, [10]; Kontoe et al., [11, 12]; Baziar et al., [13]; Bilotta et al., [14]; to research the action of underground infrastructures beneath dynamic loading.

From Lin Li et al., [15], Wenchuan earthquake that occurred in China in 2008, many tunnels damaged hardly. Longxi Tunnel on Dujiangyan-Wenchuan highway in (Figure 1) consider an indicative seismic damaged tunnel. The tunnel's fundamentally involvement three kinds of damage: (1) Longitudinal lining crack, (2) Inclined lining crack, and (3) Local lining failure. The lining cracks regarding 2-3 mm wide, distributed around the fault. (Figure 1(a)) shows the local failure that occurred on the tunnel vaults and spandrels. Furthermore, lining disturbance was also noted because of the huge shear force resulting from faulting (Figure 1(b)).

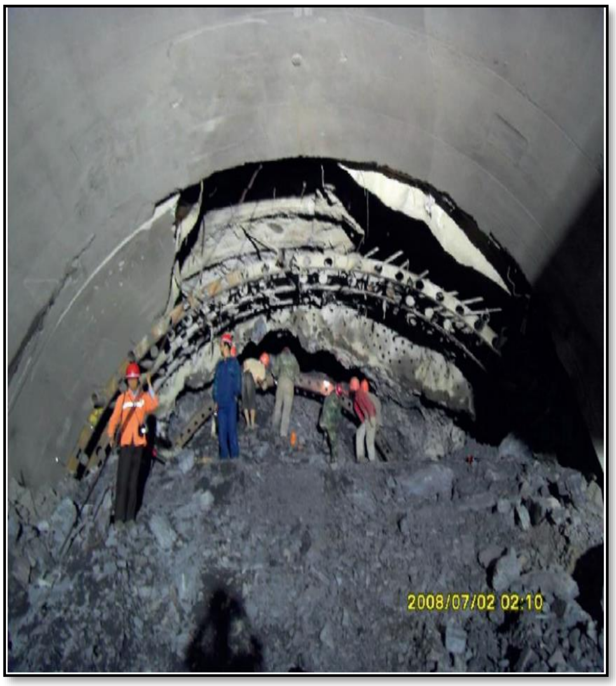


(a)

(b)

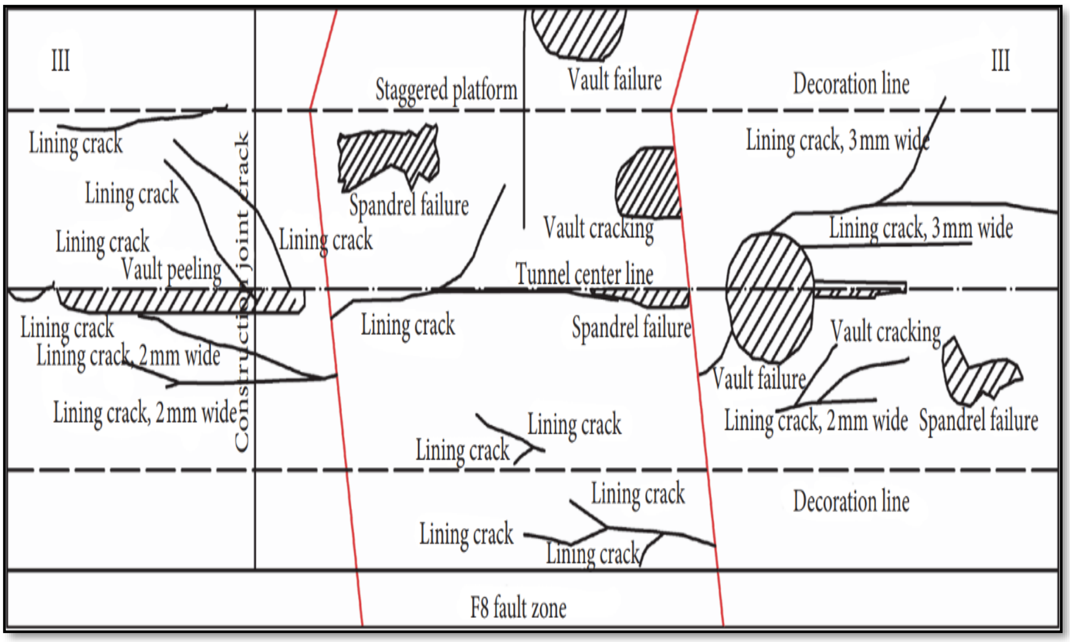


(c)

**Figure 1.** Seismic damage of Longxi Tunnel. (a) Lining collapse. (b) Lining dislocation. (c) Damage near the fault zone

## 2. General procedure of modeling

The popular modeling technique with PLAXIS is to determine the geometry with elements and materials, define the loads and boundary conditions, and make a FEM mesh, determine the initial conditions, and perform FEM calculations that consist of staged constructions.

The objective of analyzing each project is to form a geometric model which is a true three-dimensional representation, formation of points, lines, and clusters by separating the subsoil into layers, structural components, loading, and building phases. The methodology of study is shown in Figure 2.

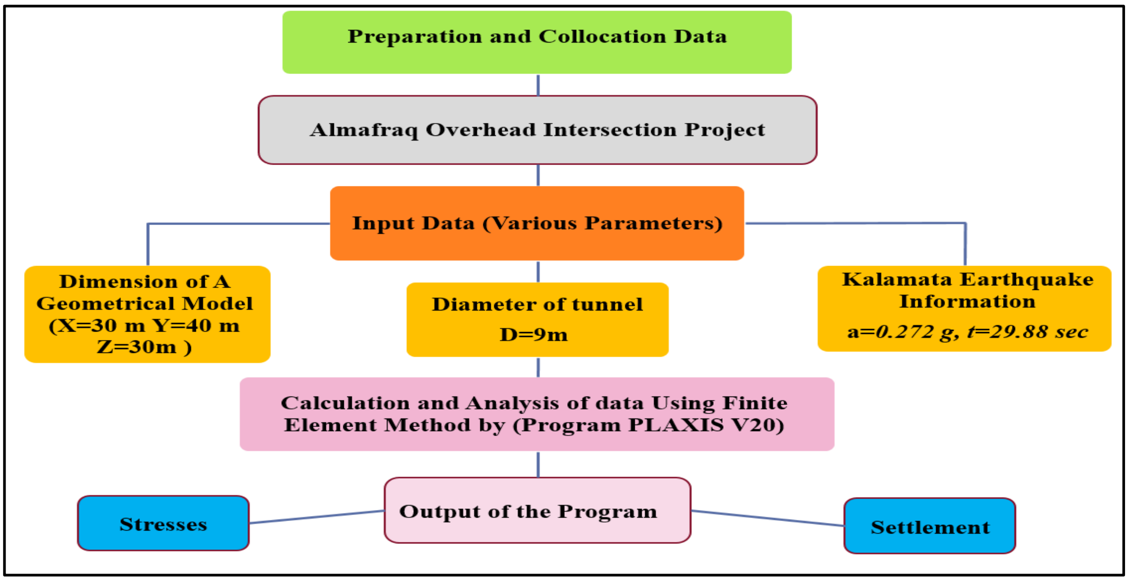


**Figure 2.** Flowchart of methodology of research

## 3. Case study

The purpose of the numerical analysis of a mechanical tunnel model is that it takes into consideration the large number of processes completed through tunnel simulation and earthquakes on it. The 3D object model includes several different components such as soil parameters, soil layers, tunnel, tunnel liner application, and earthquake parameters, all of these parameters are analyzed and simulated in the 3D FEM model.

### *3. 1. Model dimensions and soil properties*

Tunnel construction simulation is performed using FEM. The tunnel diameter (D) is assumed 9m. The type of this tunnel is a shallow tunnel. The geometry of the tunnel and the estimated network are shown in Figure 3. The support system for this tunnel was performed by placing lining with concrete to retain the tunnel steady and this type of support is considered permanent.

The simulation of tunnel construction is implemented by using FEM, and because of the symmetric model, for calculations, several solutions occupy half of the tunnel models. The diameter of the tunnel (D) supposes 9 m and its length is 40 m. The geometrical of the tunnel is represented in Figure 2. The tunnel's model depends on the real datum of soil properties of the Almafraq overhead intersection project in the Diyala government. The parameters that were gained from fundamental experiments on the soil borehole for the project and also from Bowles [16], as part of the parameters are adopted. Furthermore, the water level is set at 1.25m at the surface of soil.

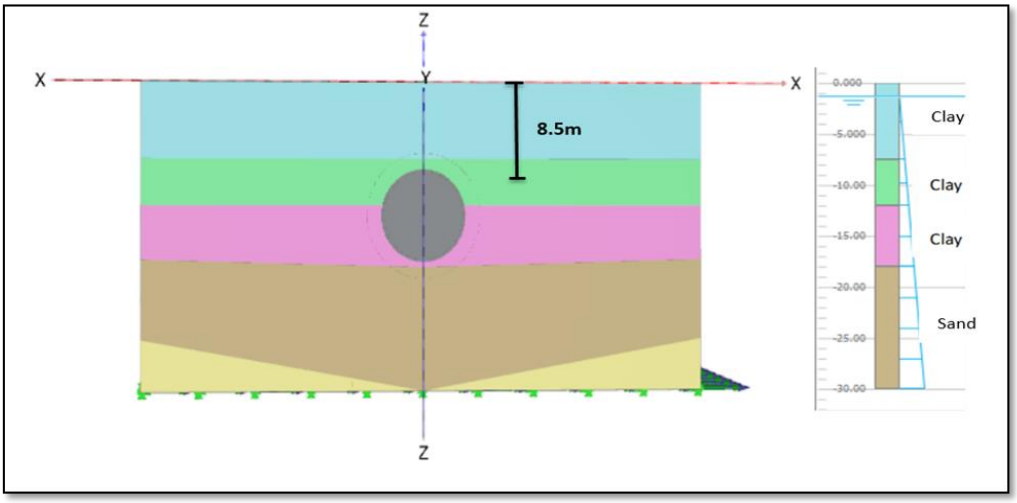


**Figure 3.** The geometry of the tunnel for the 3D model

The tunnel model is based on actual property soil data. The data obtained from the field and laboratory tests of the project are presented in Table 1. In this study, the model that describes soil behavior is the Mohr coulomb (MC) model. The properties of soils refer to clay soil.

**Table1:** The soil parameters of Mohr-Coulomb model (MC)

| Depth (m) | | Saturation unit weight of soil (kN\m³) | Unsaturation unit weight of soil (kN\m³) | Young's modulus ×103 * (kN\m²) | Cohesion (kN\m²) | Friction angle Degree (o) | Poisson's Ratio * |
|---|---|---|---|---|---|---|---|
| From(m) | To (m) | | | | | | |
| 0.0 – | 7.5 | 19.87 | 15.32 | 25 | 45 | 0 | 0.4 |
| 7.5 – | 12 | 20.8 | 16.14 | 25 | 40 | 0 | 0.4 |
| 12 – | 18 | 20.13 | 15.7 | 50 | 90 | 0 | 0.4 |
| 18 – | 30 | 19.33 | 15.7 | 80 | 1 | 41 | 0.25 |

*** (Bowles 1996)**

**Table2:** The material properties of the concrete lining element

| Parameter | Unit | Concrete Lining |
|---|---|---|
| Thickness | Meter | 0.25 |
| Unite Weight | kN/m3 | 24 |
| Possion's Ratio | - | *0.15 |
| Young's Modules | kN/m2 | $23.5\times10^6$ |

***(Bowles, 1996)**

*3.2. Input ground motion characteristics*

To estimate the seismic performance of the tunnel and the surrounding soil, the main destructive earthquake used for this case study is the Kalamata earthquake, it's an intensity of 0.272g and duration of 29.88sec. The spectral accelerations are shown in Figure 4. The earthquake is placed at the base of the soil in the x-direction in which displacement in the x-direction is prescribed and, in both y, and z direction is fixed.

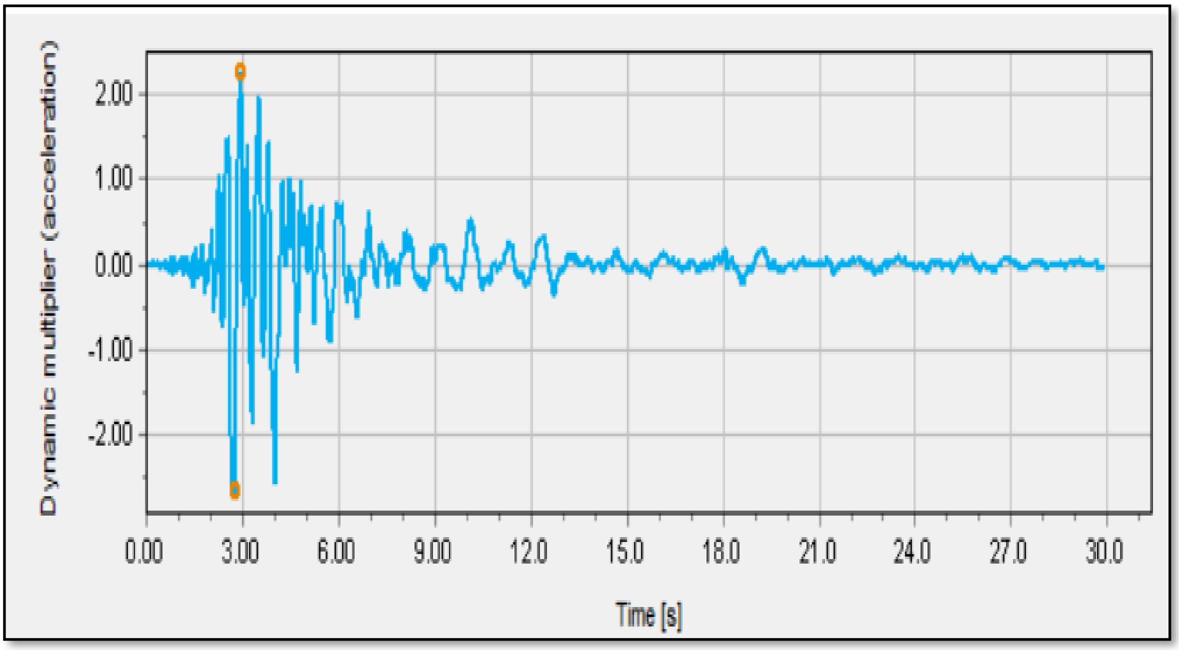


**Figure 4.** The spectral accelerations of Kalamata earthquake

*3. 3. Type of element used in numerical study*

To gain precision in engineering troubles (geotechnical troubles), the grid used for the three-dimensional finite element is the tetrahedral elements 10-node which are also used for tunnel lining modeling [17], as shown in Figure 5. Functions of the form Ni have the size of a function equal to unity at node i and zero at other nodes. The interface elements combine pairs of nodes that match the 6-point trigonometric side of the plate element or the soil element.

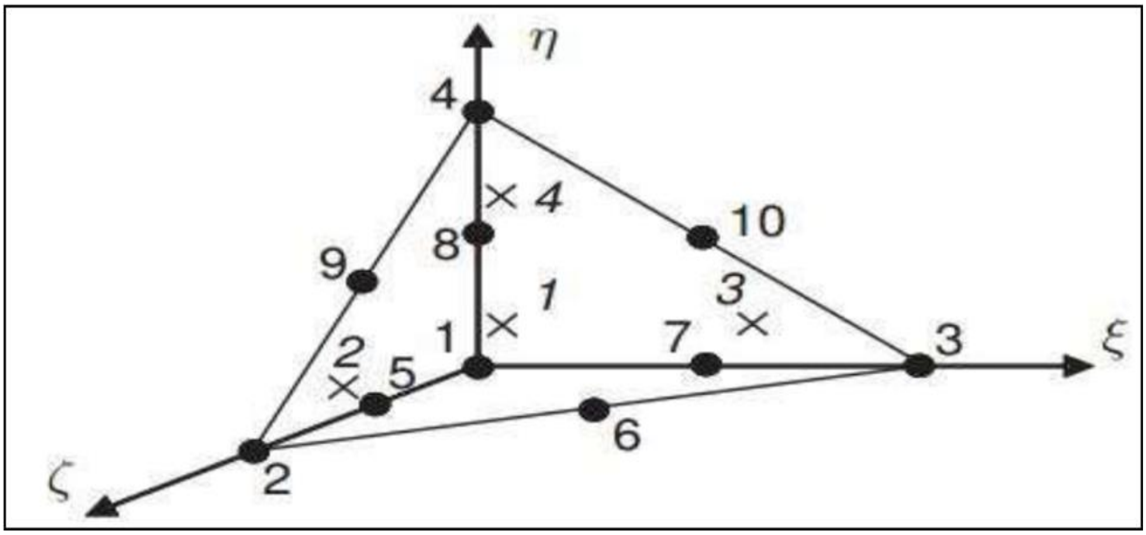


**Figure 5.** Local numbering and location of nodes (•) and integration points (x) of tetrahedral elements shape. (Brinkgreve et al, 2013)

*3. 4. Mesh Generation*

Unstructured mesh is utilized in PLAXIS 3D, which is founded automatically and is likely to adopt for local and global mesh perfection. PLAXIS 3D presents five options for the expansion of mesh density from very coarse mesh to very fine mesh. In this research coarse mesh is utilized because the mesh size needs to be relative to member size and the tunnel has many of nods so the calculation process will be so hard if we select a finer mesh. Mesh has been reduplicated in zones where stresses and strains have been predictable to be strong and crucial i.e., Figures 6 represents the tunnel, tunnel lining, and the surrounding soil of the project.

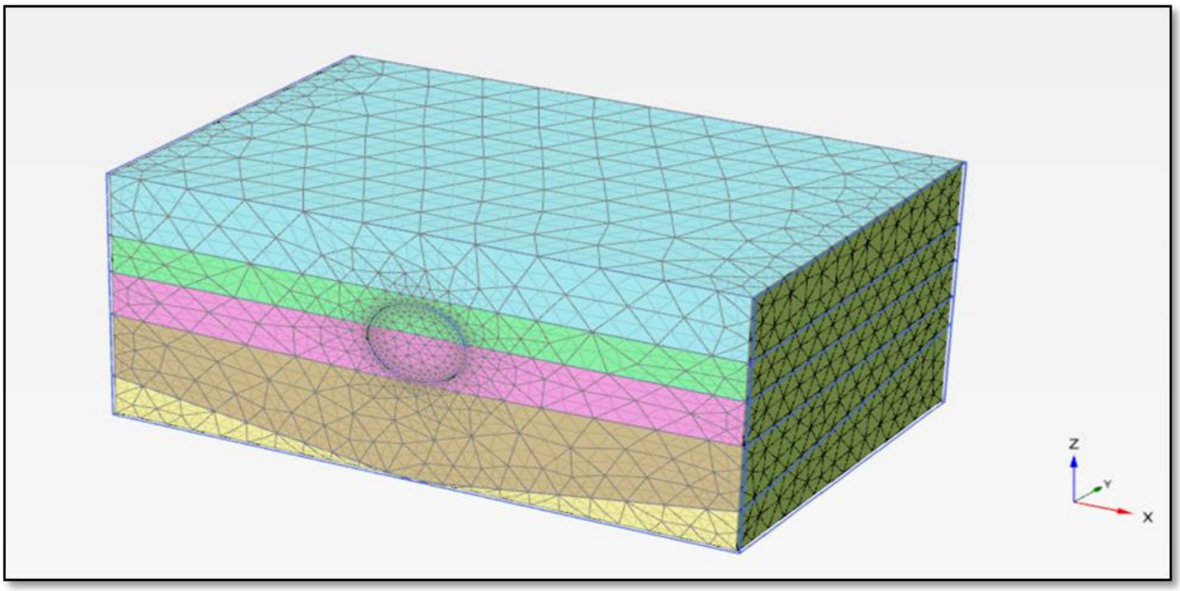


**Figure 6**. Coarse type mesh of 3D geometrical of the tunnel for (MC) model

## 4. Results and discussion of numerical model

The modeling process is composed of modeling of tunnel and exposure to the earthquake and the surrounding soil and thus displayed in two phases. The Mohr-Coulomb (MC) model is employed to demonstrate the behavior of soil-structure interaction in a soil tunnel and the soil failure criteria from the results gained. The tunnel model position appears by taking sections in the x-direction, as displayed in Figure 7.

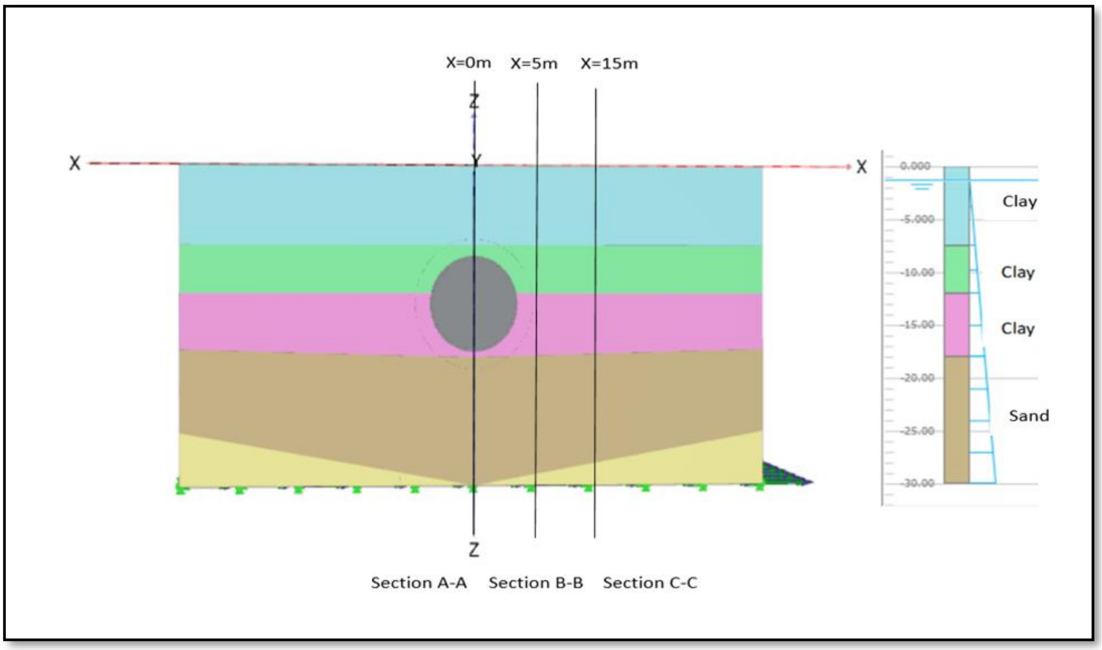


**Figure 7**. Displaying location of sections taken tunnel model at x-direction

*4.1 Stresses of section A-A*

The datum of the middle of the tunnel at X=0 and y-direction =20 is performed in this section. Figure (8) and Figure (9) display the total and effective native stress-depth curves and pore water, the behavior of the vertical stresses is comparable, and this marks a stable unit weight through the depths, while the horizontal stresses seem a variation from a depth of 20m because of the diversity in the soil layers (from clay to sand).

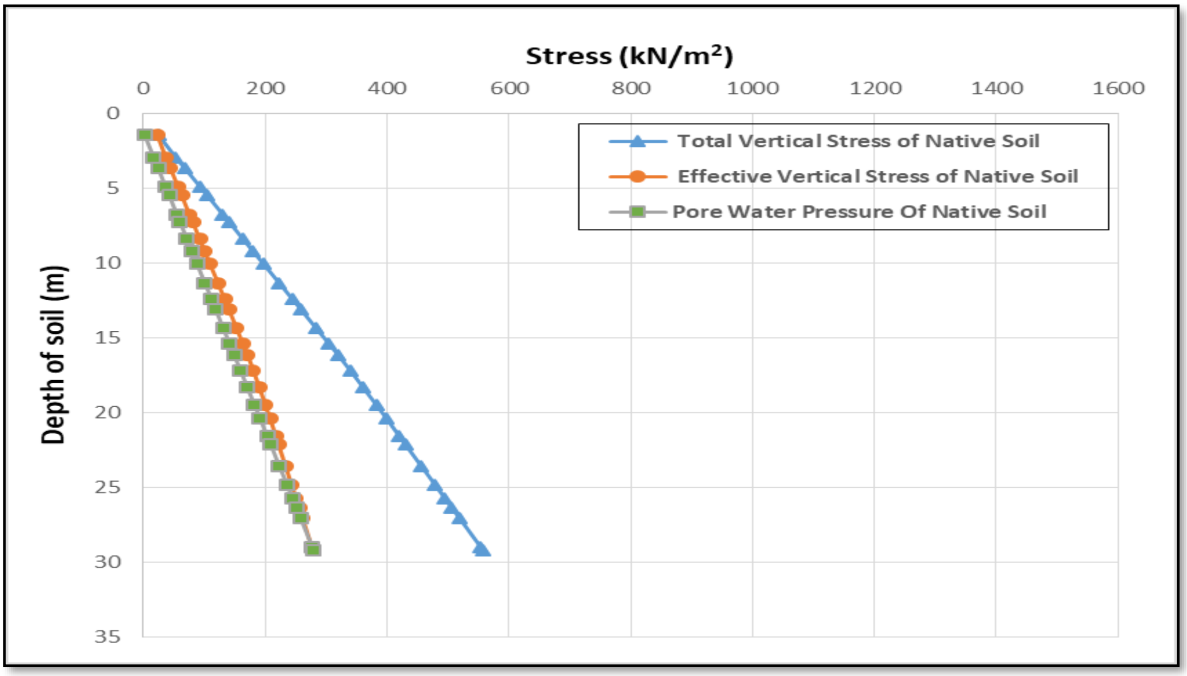


**Figure 8**. Distribution of the vertical stresses of native soil

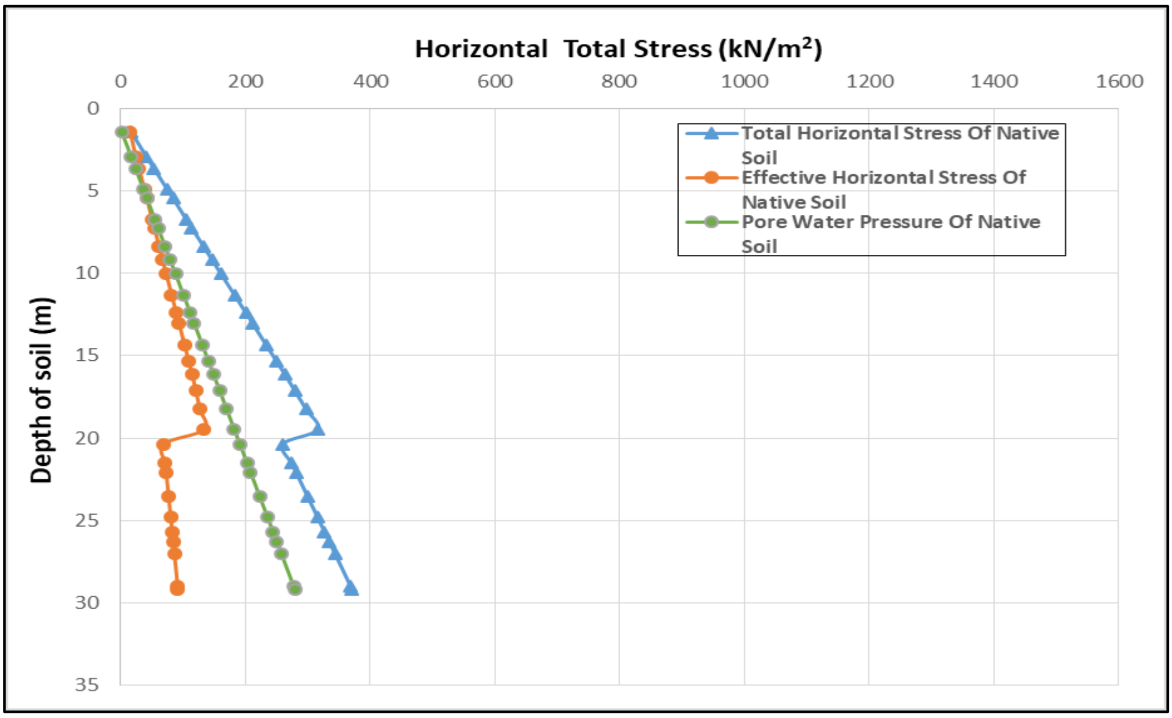


**Figure 9**. Distribution of the horizontal stresses of native soil

The stresses surrounding tunnel zone:

i. Section A-A

In the tunnel phase, at the top and bottom region of the tunnel, the total vertical stress-depth curves are comparable to the native soil with few divergence near the tunnel zone that appears to a decrease in values in 19%, while in the earthquake phase, the total and effective vertical stress-depth curves at the top region of the tunnel a comparable to the native soil with few divergence near the tunnel zone which appears to an increase in values in 26% while the lower region of the tunnel the stresses differ randomly in decrease and increase amount faraway of the native soil stresses. The total horizontal and effective stress-depth curves of the tunnel phase are visible which have a little different since the stresses become high in value both in the top in 46% and below the zone of the tunnel and become comparable at the end depths of the lower zone of the tunnel in 7%. Also, in the earthquake phase, the total horizontal and effective stress-depth curves show that the stresses have a large difference from the native soil where its values decrease at the surface and at top of tunnel in 88% and thus applicable to the lower zone of the tunnel, as shown in figures 10 and 11.

The water pressure division with depth is represented in figures 12, it is observed that pore water pressure has no larger variation (identical) in the tunnel phase, unlike that in the earthquake phase which shows a noticeable difference from the native soil in pore water pressure in 90%. No divergence is established for the tunnel phase because variations have taken place amidst total and effective whether in vertical or horizontal stresses. The difference in pore water pressure is seen in the earthquake phase at the top region and some of the lower regions and becomes comparable with the native soil in the residual region. The arise of pore water pressure is concerned with the value of water amidst particles of the soil which decrease at depths on the top region of the tunnel because it is clay layers and increases at the depths below the tunnel because it is a sandy layer, and permeability of a soil is rise for the sandy layer unlike the state in the clay layer.

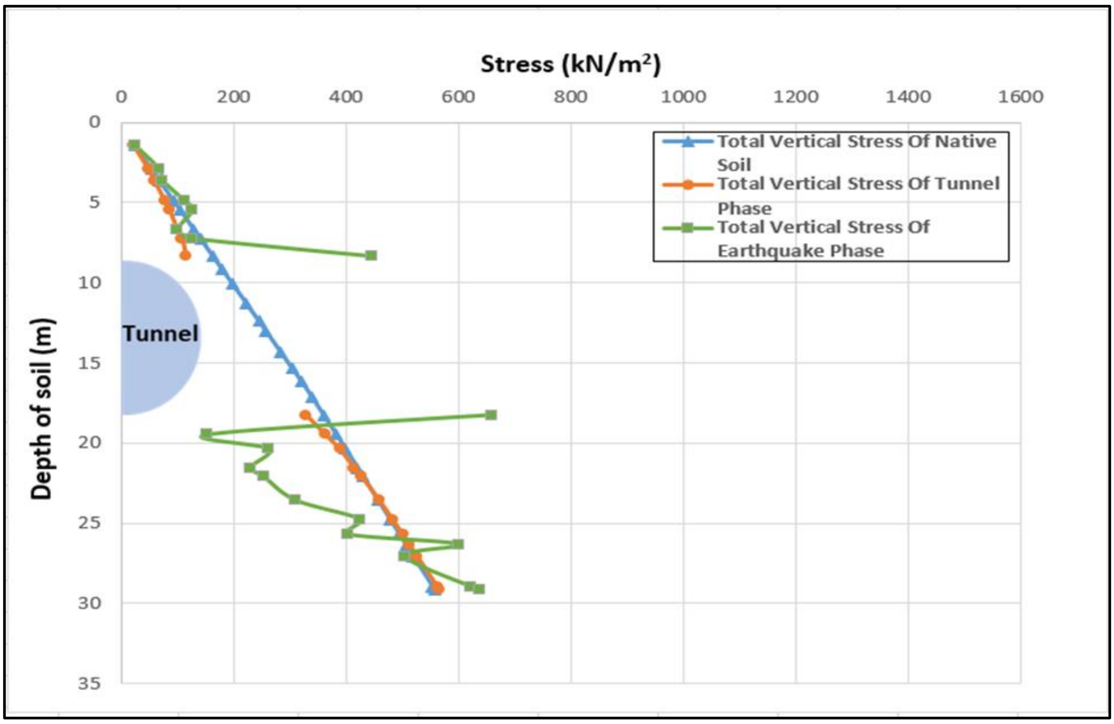


**Figure 10.** Distribution of the total vertical stresses during tunnelling phase and earthquake phase at x=0

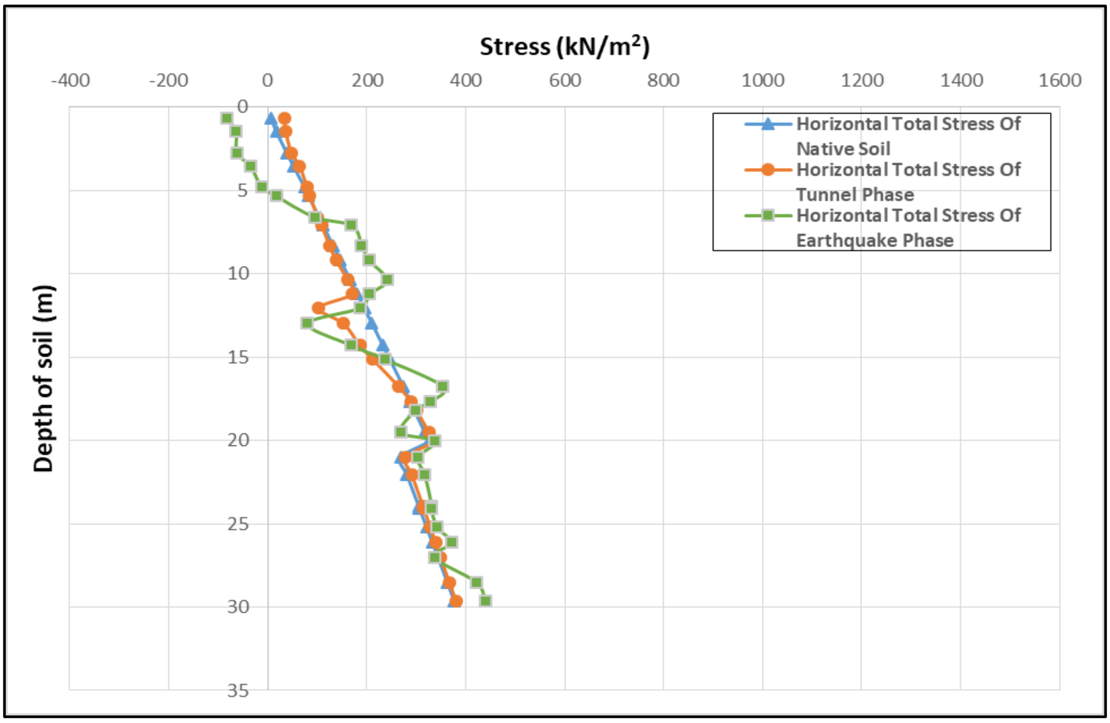


**Figure 11.** Distribution of the total vertical stress during tunnelling phase and earthquake phase at x=5 with find deviations

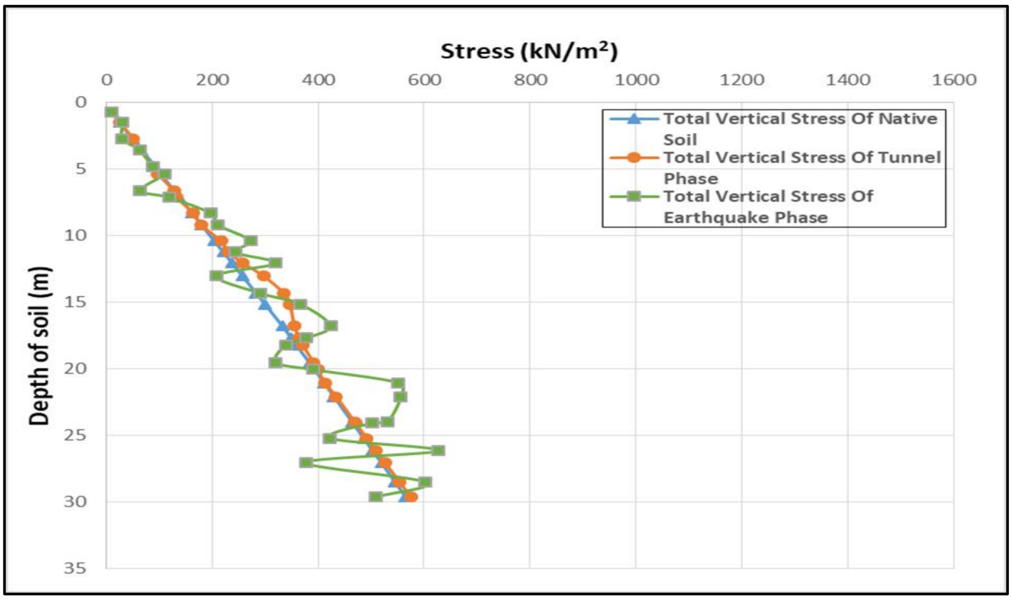


**Figure 12.** Distribution of the total horizontal stress during tunneling phase and earthquake phase at x=5 with find deviations

ii. Section B-B

This position performs the datum at various depths when y-direction =20 with deviations and x-direction =5m with several deviations. It is noteworthy that the curves of stress-depth in this status at x-direction =5 is extremely close to the tunnel region and the edge of the diameter for the tunnel end at x=4.5m. Figure 13 illustrates that the total vertical stress-depth curve of the tunnel phase are somewhat the same as native soil in value of stresses except for the zone of the tunnel since we notice an increase in its value in 7%, While in the earthquake phase the total vertical stresses at the top region of the tunnel is somewhat the same with the native soil and near the tunnel zone start increase in 8% and decrease in its value in 9%, till reach under the tunnel zone become randomly it is value differs than native soil, this randomly changer refers to the sandy layer since the permeability of a soil is rise for the sandy layer unlike the state in the clay layer.

Figure 14 illustrates that the total horizontal stress-depth curve of the tunnel phase are somewhat the same as native soil in value of stresses except for the zone of the tunnel since we notice an decrease in its value in 18% because this zone is a far from the digging zone, in expressions of depth (z) is outmost from the tunnel zone too distance (x) from its edge of the tunnel, While in the earthquake phase the total vertical stresses at the top region of the tunnel is somewhat less than the native soil in 61% and near the tunnel zone start increase and decrease in its value, till reach under the tunnel zone become greater it is value than native soil in 7%. In figure 15, it is observed that pore water pressure has no larger differences (identical) in the tunnel phase, in contrast, the earthquake phase shows a noticeable difference from the native soil in pore water pressure since the value of pore water pressure decrease in its value in 90% at the top region of the tunnel and starts to increase as much as reach tunnel region in which become near probably with the native soil and become comparable exactly at the lower zone of the tunnel.

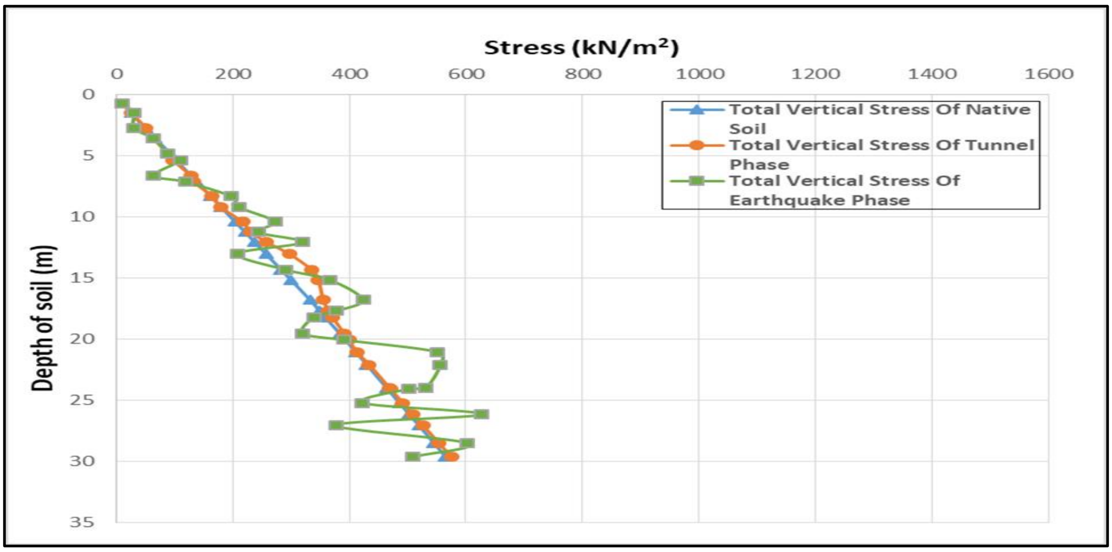


**Figure 13.** Distribution of the total vertical stress during tunneling phase and earthquake phase at x=5 with find deviations

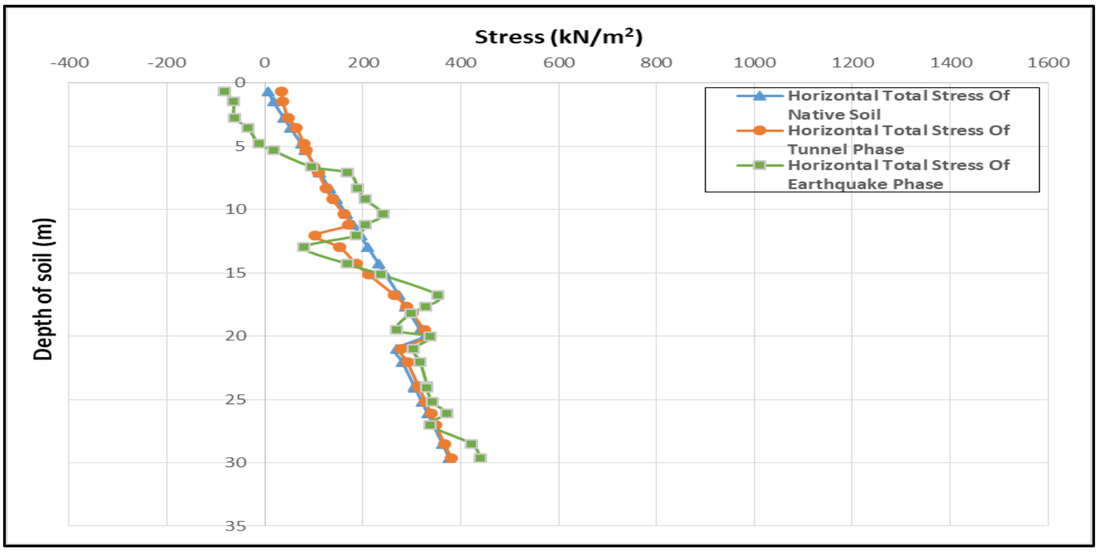


**Figure 14.** Distribution of the total horizontal stress during tunneling phase and earthquake phase at x=5 with find deviations

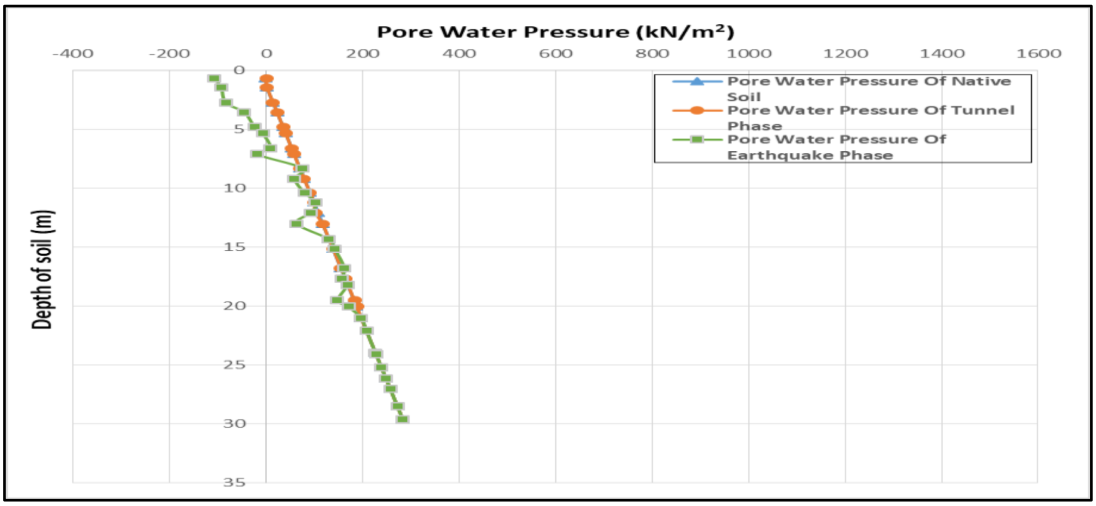


**Figure 15.** Distribution of the pore water pressure during tunneling phase and earthquake phase at x=5 with find deviations

iii. Section C-C

This position performs the datum at various depths when y-direction =20 with deviations and x-direction =15m with several deviations, which performs the datum of faraway space from the tunnel region. Furthermore, it is noteworthy that the curves of stress-depth in this status at x-direction =15 is far from the tunnel region, and the edge of the diameter for the tunnel end at x=4.5m. The total and effective stresses has shown behavior obviously which is the same behavior for native soil in the tunnel phase but is different in the earthquake phase. While the stresses- depth curves of stresses in the earthquake phase can be seen that they are different from the native soil since the stresses increase and decrease randomly to the native soil on all the tunnel zones in 12% and 21% and that happens because of the progression of seismic waves which is applied at the base, refer to figures 16 and 17. It is observed that pore water pressure effect is consider comparable with section (B-B) with a little variation as shown in Figure 18.

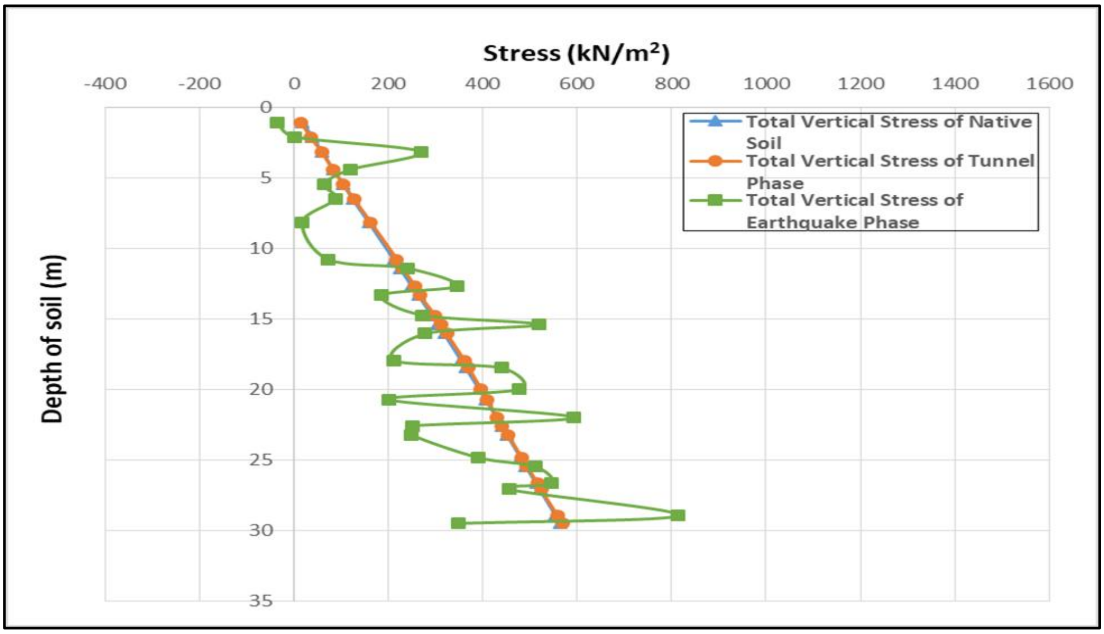


**Figure 16.** Distribution of the vertical total stress during tunneling phase and dynamic phase at x=15 with find deviations

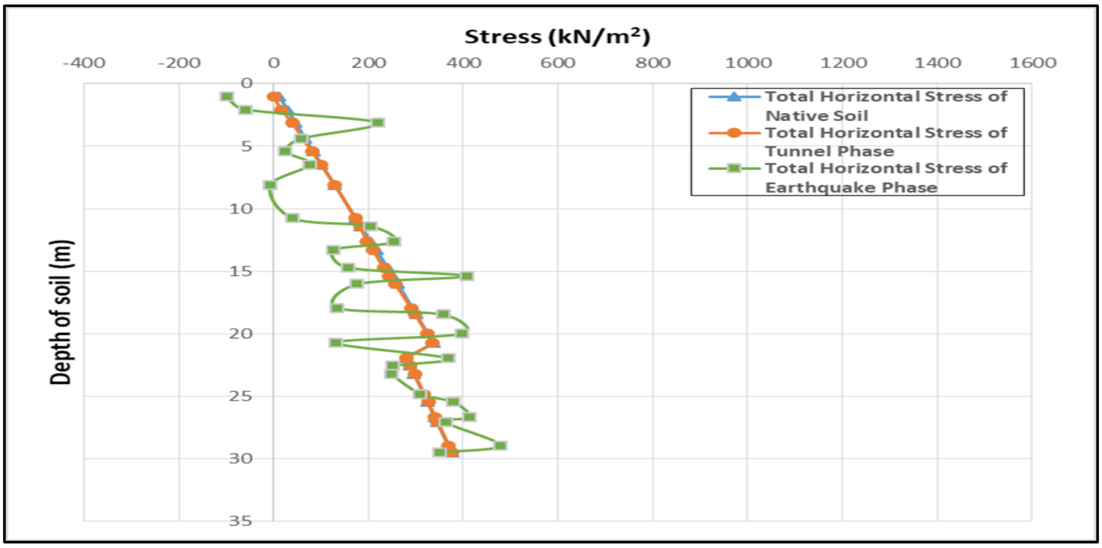


**Figure 17.** Distribution of the horizontal total stresses during tunneling phase and dynamic phase at x=15 with find deviations

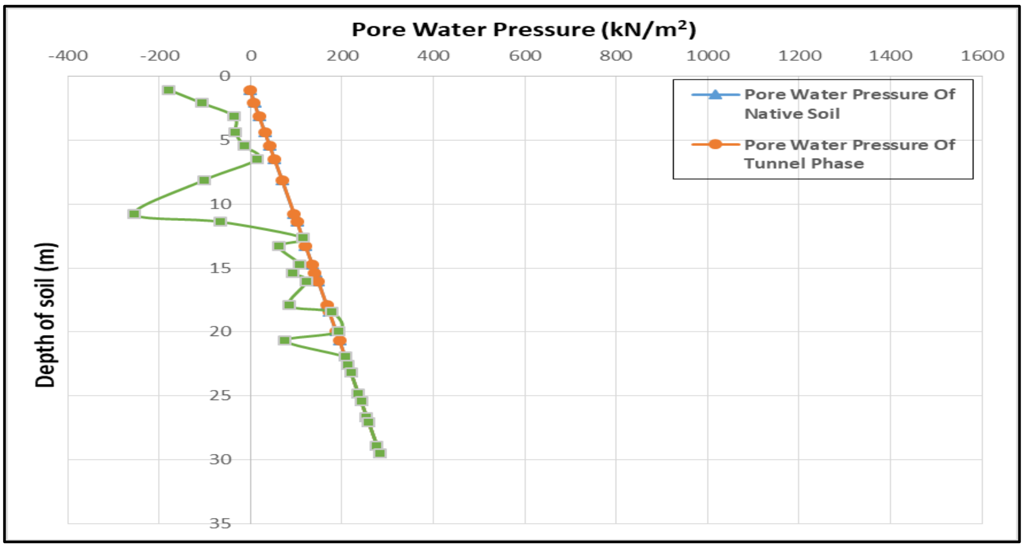


**Figure 18.** Distribution of the pore water pressure during tunneling phase and dynamic phase at x=15 with find deviations

*4.2 Surface settlement at side of tunnel boundary of the tunnel zone*

Ground movements in all directions of tunnels guide surface landing. The appreciation for settlements of the two phases through the tunnelling phase and earthquake phase is done by taken section at the surface in z-direction =0 and in y-direction =20, so it noted that the amount of the settlement of the soil is so little in a phase of tunnelling compared within the dynamic. The magnitude of maximum displacement in the vertical and the horizontal direction of all phases are shown in the Tables (3) and (4).

**Table 3:** Magnitude of maximum displacement in vertical direction of all phases

| Phases of the tunnel construction | Maximum of total displacement in vertical direction UZ (mm) |
|---|---|
| First phase | 0.003 |
| Second phase | 12 |

**Table 4:** Magnitude of maximum displacement in horizontal direction of all phases

| Phases of the tunnel construction | Maximum of total displacement in vertical direction UX (mm) |
|---|---|
| First phase | 0.01 |
| Second phase | 59 |

## 5. Conclusions

The analysis of this study concentrates quite on the variation in the state (pressure) in the case of tunnelling and earthquake effect on the soil. So, the whole curves displayed in this research point to soil stress status for pre-drilling (native soil status) with soil stress during tunnelling and earthquake phases. These modifications are recorded with regard to site status at (x = 0, x = 5, x=15). So, this makes a point as follows:

1. In the tunnel region the stresses value is large in both tunnelling and dynamic phases because of the digging process and shaking of an earthquake to the soil layer, and those values start to decrease or disappear as much as we went far away from the tunnel zone. The stresses at section x = 5 consider high when we compare it with section x = 15 since it becomes disappear as a result of the far distance from the tunnel. It was observed that the most probable safe distance (2D) from the tunnel, which D represents the diameter of the tunnel. All those stresses assemble with native soil stresses.

2. The ultimately recorded settlements are 0.003mm in the tunnel phase while in the dynamic phase is 12mm, so we notice the big differences in the effect between the two phases on the soil reach to 86% and its location above the tunnel with dimension (x=0).

## References


[1] A. Naseem, M. Kashif, N. Iqbal, K. Schotte, & H. De Backer, "Seismic behavior of triple tunnel complex in soft soil subjected to transverse shaking," *Applied Sciences*, *10*(1), 334, 2019.

[2] M. Saleh Asheghabadi, & M. Rahgozar, A, "Finite element seismic analysis of soil–tunnel interactions in clay soils," *Iranian Journal of Science and Technology, Transactions of Civil Engineering*, *43*(4), 835-849, 2019.

[3] J. Wang, "Seismic Design of Tunnels," A State-of-the-Art Approach, Monograph, Monograph 7; Parsons, Brinckerhoff Quade Douglas Inc.: New York, NY, USA, 1993.

[4] J. Penzien, "seismically induced racking of tunnel linings," Earthq. Eng. Struct. Dyn. 29, 683–691, 2000.

[5] A. Bobet, "Drained and undrained response of deep tunnels subjected to far-field shear loading," Tunn. Undergr. Space Technol. 25, 21–31, 2010.

[6] Y. M. A. Hashash, D. Park, J. I. C. Yao, "Ovaling deformations of circular tunnels under seismic loading," an update on seismic design and analysis of underground structures. Tunneling and Underground Space Technology, Vol. 20, Issue 5, p. 435-441, 2005.

[7] H. Huo, A. Bobet, J. Fernández, Ramírez," Load transfer mechanisms between underground structure and surrounding ground," evaluation of the failure of the Daikai station. Journal of Geotechnical and Geoenvironmental Engineering, Vol. 131, Issue 12, p. 1522-1533, 2005.

[8] I. Anastasopoulos, N. Gerolymos, V. Drosos, R. Kourkoulis, T. Georgarakos, G. Gazetas, "Nonlinear response of deep immersed tunnel to strong seismic shaking," Journal of Geotechnical and Geoenvironmental Engineering, Vol. 133, Issue 9, p. 1067-1090, 2007.

[9] I. Anastasopoulos, N. Gerolymos, V. Drosos, T. Georgarakos, R. Kourkoulis, G. Gazetas, "Behavior of deep immersed tunnel under combined normal fault rupture deformation and subsequent seismic shaking," Bulletin of Earthquake Engineering, Vol. 6, Issue 2, p. 213-239, 2008.

[10] A. Amorosi, D. Boldini, "Numerical modeling of the transverse dynamic behavior of circular tunnels in clayey soils," Soil Dynamics and Earthquake Engineering, Vol. 59, Issue 6, p. 1059-1072, 2009.

[11] S. Kontoe, L. Zdravkovic, D. Potts, C. Mentiki, "On the relative merits of simple and advanced constitutive models in dynamic analysis of tunnels," Geotechnique, Vol. 61, Issue 10, p. 815-829, 2011.

[12] S. Kontoe, V. Avgerinos, D. M. Potts, "Numerical validation of analytical solutions and their use for equivalent-linear seismic analysis of circular tunnels. Soil Dynamics and Earthquake Engineering, Vol. 66, p. 206-219, 2014.

[13] M. H. Baziar, M. R. Moghadam, D.-S. Kim, Y. W. Choo, "Effect of underground tunnel on the ground surface acceleration," Tunneling and Underground Space Technology, Vol. 44, p. 10-22, 2014.

[14] E. Bilotta, G. Lanzano, S. P. G. Madabhushi, F. Silvestri, "A numerical Round Robin on tunnels under seismic actions," Acta Geotechnica, Vol. 9, Issue 4, p. 563-579, 2014.

[15] J. E. Bowles, "Foundation Analysis and Design," Fifth edition, McGraw-Hill International book company, Tokyo, Japan, (1996).

[16] R.B. J Brinkgrever, "Finite Element Code for Soil and Rock Analysis," User Manual Plaxis 3D. Version 2013. The Nederland's, Delft University of Technology by Plaxis V20, 2008.